Mat. Res. Soc. Symp. Proc. Vol. 705 © 2002 Materials Research Society

High Density Hexagonal Nickel Nanowire Arrays with 65 and 100 nm-PERIOD

Kornelius Nielsch[1], Ralf B. Wehrspohn[1], Saskia F. Fischer[2], Helmut Kronmüller[3], Jochen Barthel[1], Jürgen Kirschner[1], Thomas Schweinböck[4], Dieter Weiss[4] and Ulrich Gösele[1].
[1]Max-Planck-Institute of Microstructure Physics, Weinberg 2, 06120 Halle, Germany.
[2]Department of Electronic Materials, Ruhr-Universität-Bochum, Lehrstuhl für Werkstoffe der Elektrotechnik, 44780 Bochum.
[3]Max-Planck- Institute of Metal Research, Heisenbergstr. 1, 70569 Stuttgart.
[4]Thomas Schweinböck und Dieter Weiss, Institute of Applied Physics, University of Regensburg, Universitätsstr. 31, 93040 Regensburg, Germany.

ABSTRACT

Highly ordered alumina pore channel arrays are used as templates for the fabrication of magnetic nanowire arrays. These well-defined templates are based on the approach by Masuda and Fukuda and have an interpore distance of 65 and 100 nm and a monodisperse pore diameter of ≈30 nm. The pore channels are hexagonally arranged in 2D-domains, which extend over more than ten interpore distances. Nearly 100% metal filling of the alumina pore structures is obtained by a novel pulsed electrodeposition technique. Due to the high ordering degree of the nanowires arrays, we detect a squareness of ≈100% and coercive fields of 1200 Oe in the direction of the nanowires. The MFM measurements have been carried out by applying magnetic fields on magnetized and demagnetized samples to study the switching behavior of individual nanowires inside the arrays. Magnetic wires have been locally switched by a strong MFM tip and a variable external magnetic field. The MFM results show a good agreement with the bulk magnetic hysteresis loops.

INTRODUCTION

The possibility to obtain tailored nanostructured magnetic materials has stimulated a world wide research effort towards innovative products in the fields of magnetic storage, bio-medical diagnostics and drug delivery. Patterned perpendicular storage media consisting of magnetic nanowire arrays [1-4] in a magnetically insulating matrix allow high storage densities [5]. More than 700 Gbit/in^2 areal density has been predicted for these structures. Furthermore, these nanowire arrays are very well suited for the preparation of ferrofluidic solutions containing monodisperse nanowires, which are very promising for effective cancer treatments and diagnostic methods [6]. One promising technique to obtain highly-ordered magnetic nanowire arrays is based on hexagonally arranged porous-alumina templates [5, 7-9].

Since 1981, there have been numerous studies on ferromagnetic nanowire arrays in disordered alumina templates [5,7,8]. These structures had large size distributions of the pore diameter and interpore distance and the filling degree of the pores was not specified. Based on a recent approach by Masuda [10], ordered alumina pore channel arrays can be obtained with a sharply defined pore diameter (<10%) [11,12]. The degree of self-ordering is polydomain with a

typical domain size of a few microns, i.e., more than 20 times the interpore distance. The nearly perfect pore arrangement occurs for interpore distances of D_{Int}= 65 and 100 nm with adjustable pore diameters from D_P= 25 to 70 nm. Here, we will focus on nickel as a filling material due to its negligible magneto-crystalline anisotropy, so that the inter-actions between the anisotropy resulting from the nanowire shape and the stray field inside the magnetic arrays can be studied in detail. The small magnetic moment of Ni, compared to Fe and Co, leads to low dipole interactions between nanowires [2].

SAMPLE PREPARATION

Hexagonally-ordered porous Al_2O_3 templates were first fabricated on aluminum substrates using a two-step electrochemical anodization process [10,13] (Fig. 1 **(a)**). The formation of small dendrite pores at the pore bottom promotes a homogeneous nucleation for the electrochemical deposition inside the pores **(b)** [13]. Nickel was directly plated onto the nearly insulating barrier oxide at the pore bottom from a Watts-type electrolyte and by current pulses **(c)**. This technique yields a homogeneous Ni filling of the high aspect-ratio pore channels [13]. Subsequently, Si substrates were fixed on top of the array **(d)**, the Al substrate was selectively removed by chemical etching and the sample was turned upside down **(e)**. In order to reduce the stray field interactions between the nanowires, the barrier layer and the dendrite part of the nanowires were removed by sputtering with a focused ion beam **(f)**. Transmission electron micrographs (Fig. 2a) of the nanowire structures revealed a column spacing of D_{Int}= 65 nm, and column diameter of $D_P \approx$25 nm. Samples with D_{Int}= 100 nm and D_P= 30 nm were also obtained. This TEM image shows the ferromagnetic nanowires (grey to black) with a monodisperse diameter are embedded in the porous alumina matrix (white). These fluctuations of the grey scale in the nanowire are due to the different orientations of the nanowire crystallites, which have a fcc-lattice and exhibits a tetrahedral shape. Due to the self-organization process, the nanowires are arranged in a hexagonal pattern. The fabrication of these highly ordered porous alumina template filled with nanocyrstalline ferromagnetic materials and single crystalline silver was recently reported in detail by us in Ref. 14 and 15, respectively.

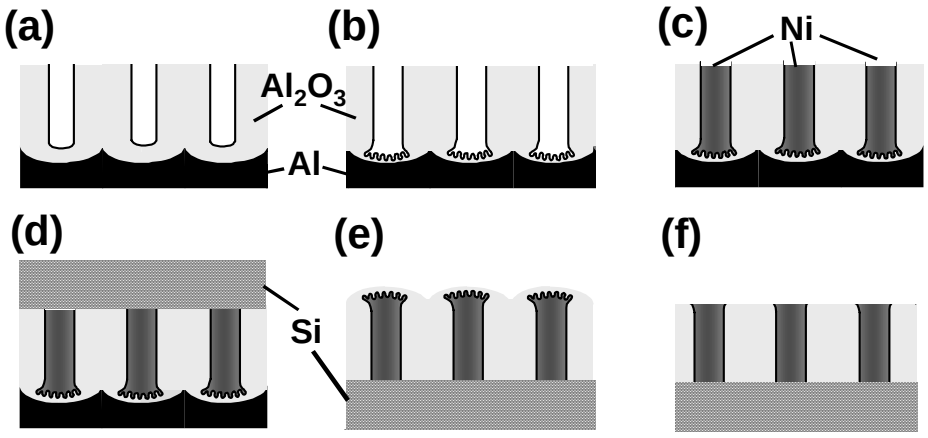

Figure. 1: Preparation steps for fabrication of highly-ordered nickel nanowire arrays embedded in an alumina matrix and fixed to a Si substrate.

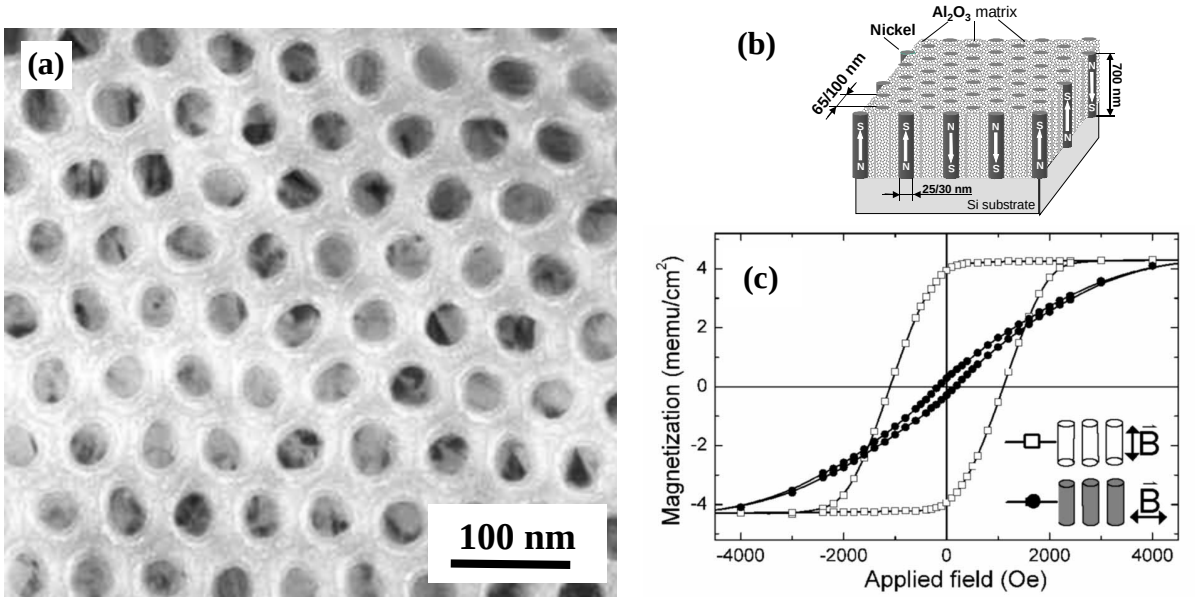

Figure. 2: TEM micrograph **(a)** and sketch **(b)** of a nickel-filled alumina matrix with an interwire distance of 65 nm. The Ni columns have a diameter of 25 nm and a length of ≈700nm. The SQUID-Hysteresis loops **(c)** of this Ni nanowire array.

EXPERIMENTAL RESULTS AND DISCUSSION

For the characterization of the bulk-magnetic properties a SQUID-magnetometer was used. Fig. 2(c) shows the hysteresis loop for the sample with D_{Int}= 65 nm and D_P = 25 nm. The measured hysteresis for an applied field parallel to the axis of the nanowires exhibits a coercivity $H_c^{||} \approx$ 1100 Oe and a squareness of 96 %. This sample has its preferential magnetic orientation along the column axis. In the perpendicular direction the coercivity is small ($H_c^{\perp} \approx 150$ *Oe),* large magnetic fields are required for a complete magnetization and the loop shows a nearly reversible behavior. As shown recently, for this arrangement each Ni nanowire is a single domain particle and its anisotropy is determined by the particle shape [8]. When this magnetic array is completely magnetized in the preferential magnetic orientation, the average internal stray field between the nanowires is $H_D^{||} = 2\pi^{3/2}(D_P/D_{int})^2 \cdot M_S$= 770 Oe [8] and thus smaller than $H_c^{||}$. Each Ni nanowire has on average a switching field $H_{sw} \approx H_c^{||}$ with a standard deviation ΔH_{sw}, due to the diameter variation. After the sample has been saturated along the nanowire axis and the magnetic field has been switched off, a very small fraction of nanowires reverse their magnetization, because locally $(H_{sw}-\Delta H_{sw}) < H_D$. This explains the small deviation of the measured squareness (96%) from the expected value of 100% for $H_D^{||} < H_C^{||}$.

For a decrease in (D_P/D_{Int}), the dipolar interactions inside the array will be reduced. Fig. 3 shows the major hysteresis loop for the sample with D_{Int}= 100 nm and D_P= 30 nm, which exhibits a slightly enhanced coercivity ($Hc^{||} \approx$1200 Oe) and squareness (100%). Due to the reduction of D_P/D_{Int}= 0.39 → 0.3, this sample has a lower demagnetization field of $H_D^{||}$ = 455 Oe. This value is considerably lower than H_{sw} of the magnetically weakest nanowires inside the array. Therefore, no nanowire should reverse its magnetic polarization after the sample has been completely magnetize. This has been observed recently by magnetic force microcopy (MFM),

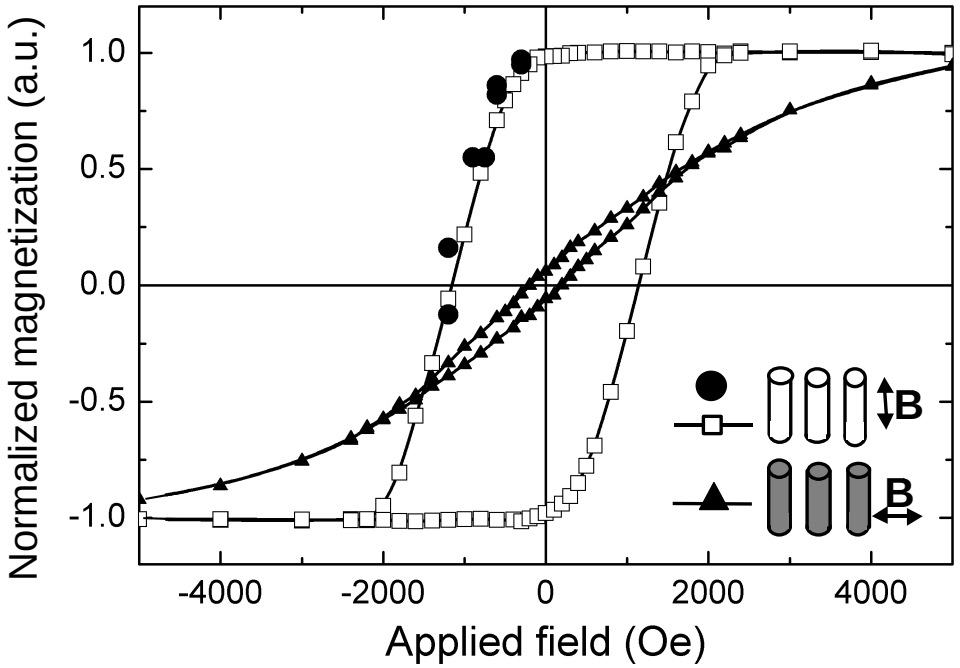

Figure 3: SQUID-Hysteresis loops of the nickel nanowire array with a pitch of 100 nm, column length of about 700 nm and a wire diameter of 30 nm measured with an applied field parallel (□) and perpendicular (▲) to the column axis. Results from MFM investigations (●) while an external magnetic field Hex was applied to the sample (statistical analysis).

too [15]. The statistical results from the analyzes of MFM images, measured in the presence of an external magnetic field, are also plotted in Fig. 3 and are in good agreement with the SQUID-results.

In order to examine in detail the suitability of this nickel nanowire array for patterned perpendicular magnetic media, we have tried to completely magnetize a defined area of a demagnetized sample by a strong magnetic MFM tip ($H_{Tip} \approx 250$ *Oe*) and an external magnetic field ($H_{ex} = -1200$ *Oe*). The amount of the applied external field was nearly equal to the average switching field (H_{sw}) of the individual nanowire ($H_{sw} \approx H_C^{//} = 1200$ *Oe*) and was applied in the direction of the nanowire axis. Starting in the upper region of Fig. 4 the strong magnetic tip was scanned over an area of $5 \times 5\ \mu m^2$. Hereby, a total external field of about $H_{ex}' = H_{ex} + H_{Tip} = -1450$ *Oe* was applied locally to the tips of the nickel nanowires. Subsequently, the external magnetic field was switched off. An enlarge area of $10 \times 10\ \mu m^2$ (Fig. 4) was scanned with the magnetic tip in order to measure the domain pattern of the manipulated area in the nanowire array. Inside the area of the first scan nearly every nickel column *(~93%)* is magnetized in the same direction.

Fig. 4 shows the local impact (dark quadratic region) of the external magnetic field and the strong magnetic tip during the first MFM scan on the magnetization of nanowires. Around the magnetized region of 5×5 µm the nickel nanowire array remained in the demagnetized state and exhibited the labyrinth-like domain pattern [9]. The border between the magnetized area and the surrounding demagnetized area is clearly visible. From the picture, it can be concluded that applied magnetic field ($H_{sw} \approx H_C^{//}$) alone was not strong enough for the switching of magnetic

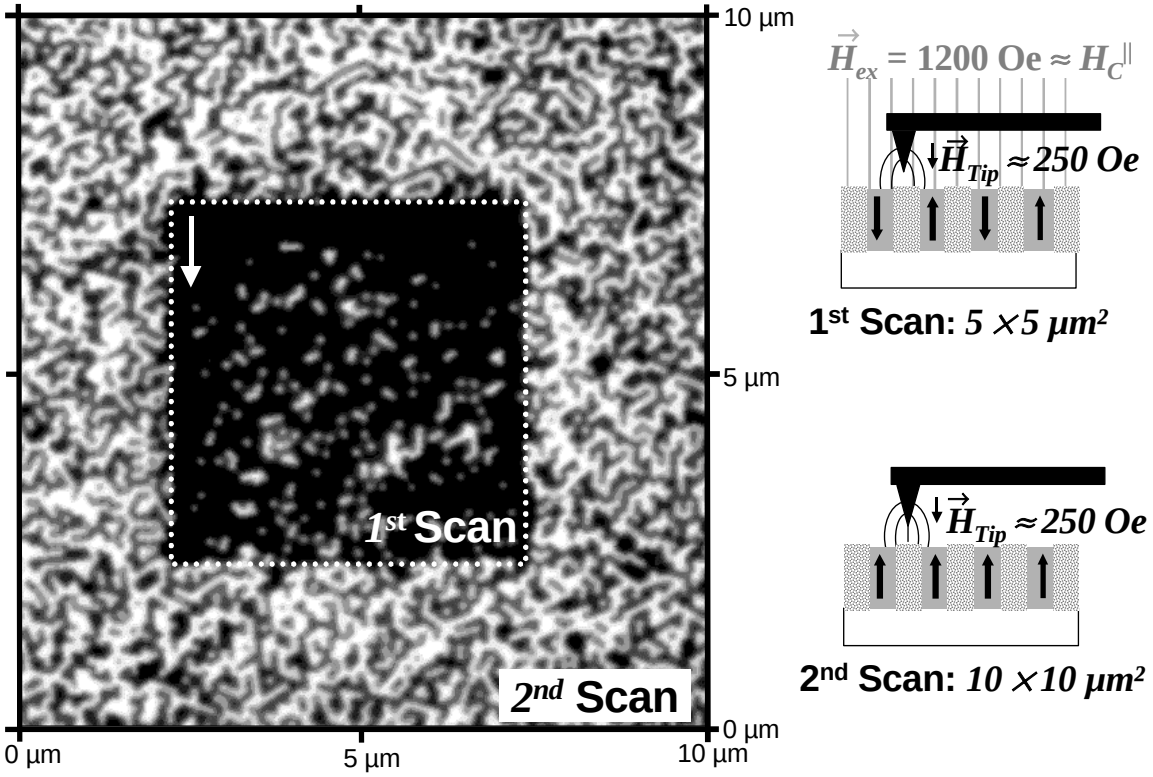

Figure 4: Local magnetic switching of a demagnetized sample area (5×5 µm^2, 1st scan) by a strong magnetic MFM tip (H_{Tip} ≈250 Oe) and an external magnetic field (H_{ex} = -1200 Oe). This image of the domain pattern (10×10 µm^2) was recorded by a second subsequent MFM scan without an external magnetic field.

polarization in the Ni columns. Hence, the additional field contribution from the strong MFM tip (H_{Tip}) enabled the local switching process in the Ni nanowire array.

The probability for a nickel nanowire to remain unswitched (light spots) increases in the lower region of the magnetically manipulated area (Fig. 4: 1st scan). In the upper region, where the first magnetic scan procedure had started, the first five or six horizontal nanowire rows have been completely magnetized in the same direction. During the first scan procedure when the area of the completely magnetized nanowires was growing, the probability for nanomagnet to remain unswitched increased. We assume that the strayfield interactions between the demagnetized and the magnetized area can be neglected and the net strayfield in the demagnetized area is zero. By increasing the area of parallel magnetized nanowires the dipole interactions between the magnetic elements are enhanced and the applied local field (H_{Tip} + H_{ex}) is getting less sufficient for a complete magnetic alignment of magnetization. At the left and right border of the magnetically manipulated area the strayfield interactions are weak and a lower number of unswitched magnetic columns is observed there. From this experiment, it can be concluded that the stray field dipole interactions between the nanowires are extended over several interwire distances due to their high aspect ratio (nanowire length to interwire distance: L/D_{INT} >7). Recent micromagnetic finite element simulations of Hertel [16,17] show that for nickel nanowires with diameters ≤ 40 nm the magnetic reversal occurs by means of a nucleation-propagation pro??cess [16]. A different reversal by means of a localised curling mode has been

reported recently for Ni nanowires with larger diameters (60 nm) [17]. These simulations are in line with our observations that the nickel nanowire ($D_P \leq 40$ nm) are single domain nanomagnets. In principle, the single nanowire can store one bit of information and can be locally switched independently to the magnetization of its nearest neighbours.

CONCLUSIONS

The measurement of the bulk-magnetic properties shows a strong magnetic anisotropy along the nickel column axes, coercive fields of 1200 Oe and nearly 100% squareness. The MFM measurements have been carried out by applying magnetic fields on magnetized and de-magnetized samples to study the switching behaviour of individual nanowires inside the arrays. Good agreement between the MFM investigation in the presence of an external magnetic field and the hysteresis loop was obtained. Magnetic wires have been locally switched by a strong MFM tip and a variable external magnetic field. Each magnetic pillar is a single domain magnetic particle, magnetised perpendicularly to the template surface and, in principle, can store one bit of information.

REFERENCES

[1] S.Y. Chou, M.S. Wei, P.R. Krauss, and P.B. Fischer, *J. Appl. Phys.* **76**, 6673 (1994).
[2] C.A. Ross, H.I. Smith, T.A. Savas, M. Schattenberg, M. Farhoud, M. Hwang, M. Walsh, M.C. Abraham, and R.J. Ram, *J. Vac. Sci. Technol.* **B17**, 3168 (1999).
[3] T. Thurn-Albrecht, J. Schotter, C.A. Kastle, N. Emley, T. Shibauchi, L. Krusin-Elbaum, K. Guarini, C.T. Black, M.T. Tuominen, and T.P. Russell, *Science* **290**, 2126 (2000).
[4] M. Zenger, W. Breuer, M. Zölfl, R. Pulwey, J. Raabe, and D. Weiss, *IEEE Trans. Magn.* **37**, 2094 (2001).
[5] S. Kawai and R. Ueda, *J. Electrochem. Soc.* **122**, 32 (1975).
[6] H. Schmidt, *Appl Organomet. Chem.* **15**, 331 (2001).
[7] D. AlMawlawi, N. Coombs, and M. Moskovits, *J. Appl. Phys.* **69**, 5150 (1991).
[8] D.J. Sellmyer, M. Zheng, and R. Skomski, *J Phys. Condens. Mat* **13**, R433 (2001).
[9] K. Nielsch, R. B. Wehrspohn, J. Barthel, J. Kirschner, U. Gösele, S. F. Fischer, and H. Kronmüller, *Appl. Phys. Lett.* **79**, 1360 (2001).
[10] H. Masuda and K. Fukuda, *Science* **268**, 1466 (1995).
[11] O. Jessensky, F. Müller, and U. Gösele, *Appl. Phys. Lett.* **72**, 1173 (1998).
[12] A.P. Li, F. Müller, A. Birner, K. Nielsch, and U. Gösele, *J. Appl. Phys.* **84**, 6023 (1999).
[13] K. Nielsch, F. Müller, A. P. Li, and U. Gösele, *Adv. Mater.* **12**, 582 (2000).
[14] G. Sauer, G. Brehm, S. Schneider, K. Nielsch, R.B. Wehrsphohn, F. Müller and U. Gösele, *J. Appl. Phys.* **91**, 3243 (2002).
[15] K. Nielsch, R.B. Wehrspohn, J. Barthel, J. Kirschner, S.F. Fischer, H. Kronmüller, T. Schweinböck, D. Weiss, and U. Gösele, *J. Magn. Magn. Mater.*, in press (April 2002).
[16] R. Hertel, *J. Appl. Phys.* **90**, 5752 (2001).
[17] R. Hertel, *J. Magn. Magn. Mater.*, in press (April 2002).